Deformation of Kobe Ohashi Bridge Foundation Caused by 1995 Great Hanshin Earthquake, Japan

by

Hanlong Liu[1], Susumu Iai[1], Koji Ichii[1] and Toshikazu Morita[1]

ABSTRACT

During the 1995 Great Hanshin earthquake, there was about 0.6 to 0.8m seaward displacement induced at the pneumatic caissons which were embedded to a depth of 33m. In order to identify the mechanism of deformation, the effective stress analysis was performed to take into account the soil-structural and water-structural interactions. The constitutive model used in this study is a multiply mechanism type defined in strain space and can take into account the effect of rotation of principal stress axis directions. The earthquake acceleration recorded at a depth of 83 meters on the Port Island during the 1995 Great Hanshin earthquake was used as input bedrock motion. The results of analysis show that the seaward residual displacements were 0.46 m at the top of a caisson and 0.48 m at the top of the other caisson, resulting in a total of 0.94m. The order of computed residual displacement was in good agreement with the measured. The results indicate that the excess pore water pressure increasing in the fill soil around the caissons and in the diluvial layers significantly affected the performance of caissons. The performance of pneumatic caisson foundation for soil improvement was also discussed.

Key Words: Kobe Ohashi Bridge, Pneumatic Caisson Foundation, Effective Stress Analysis, Liquefaction, Residual Deformation

1. INTRODUCTION

Kobe port is located in the south of Kobe city about 17 km from the epicenter of the 1995 Great Hanshin earthquake. The Kobe Ohashi Bridge, 319 meters long, with a central span 217 meter long and two-side spans 51 meter long, lies on the site between the Fourth Pier and the Port Island in Kobe port area. It is the only bridge connecting Port Island with the Kobe city. There are two pneumatic concrete caissons P2 and P3 used for the foundations to support the main span of the bridge. The location and cross section are shown in Fig.1. During the 1995 Great Hanshin earthquake, the bridge was shaken by a strong earthquake motion having the peak acceleration of 670 Gal and 172 Gal in the N-S horizontal and vertical directions at the bedrock 83m deep from the ground surface. Though the pneumatic caissons were embedded in soil to a depth of 33m and founded on a firm foundation of Holocene origin, there were about 0.60 to 0.80m residual displacements toward sea and 0.36 to 0.93 degrees angle of seaward inclination induced due to earthquake. The bridge and the damage around the bridge after earthquake was shown in Photo.1, and the relative movement between the upper structure of bridge and foundation at P2 was shown in Photo. 2. In order to identify the mechanism of the deformation for the foundation, an effective stress analysis was performed in this study based on the results of the geotechnical investigations and in-situ velocity measurements.

2.EFFECTIVE STRESS ANALYSIS

2.1 Constitutive Equations

The constitutive model used in this study is a strain space plasticity type and consists of a multiple shear mechanism in the plane strain

1) Geotechnical Earthquake Engineering Laboratory, Port and Harbour Research Institute, Ministry of Transport, 3-1-1, Nagase, Yokosuka 239, Japan
Tel: 81-468-44-5028, Fax: 81-468-44-4095

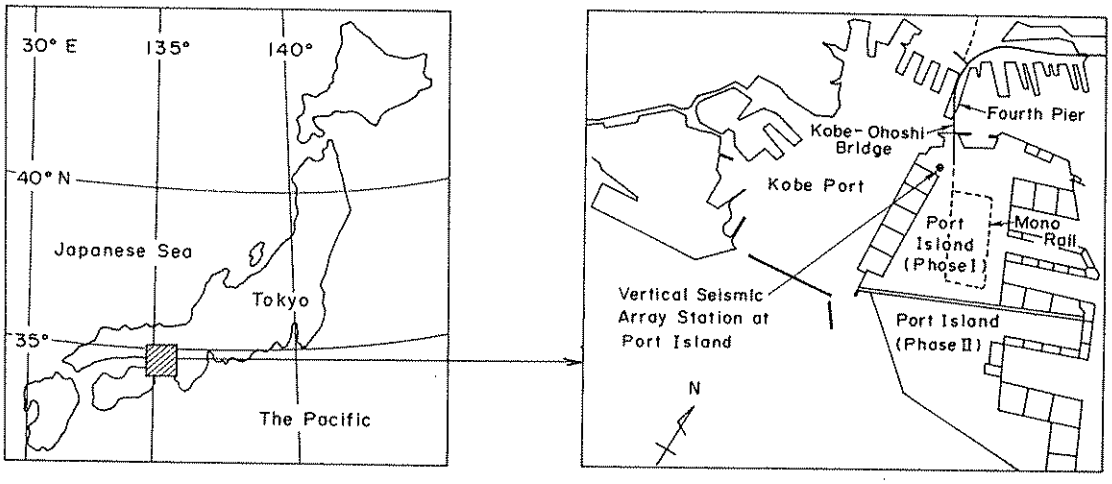

(a) Location

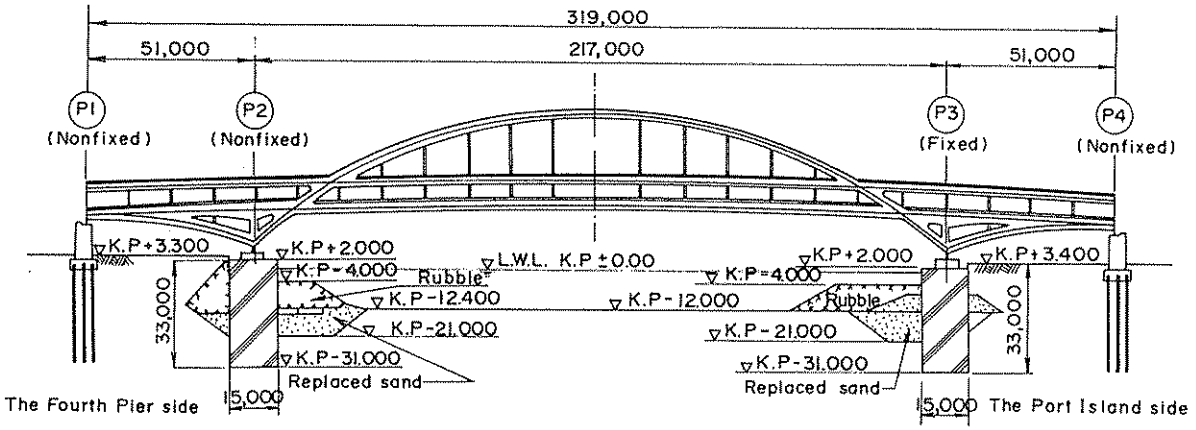

(b) Cross section

Fig.1 The location and cross section of Kobe Ohashi Bridge

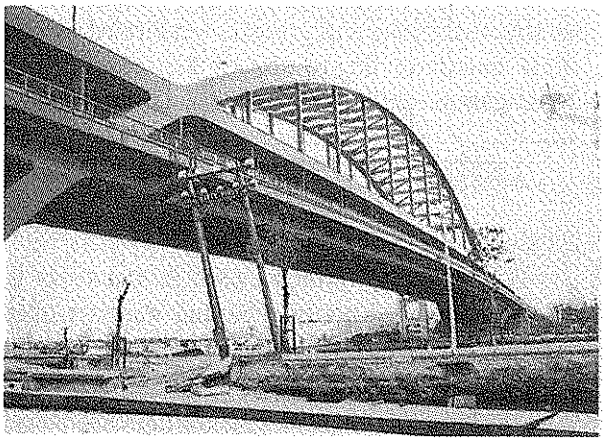

Photo 1 The Kobe Ohashi Bridge

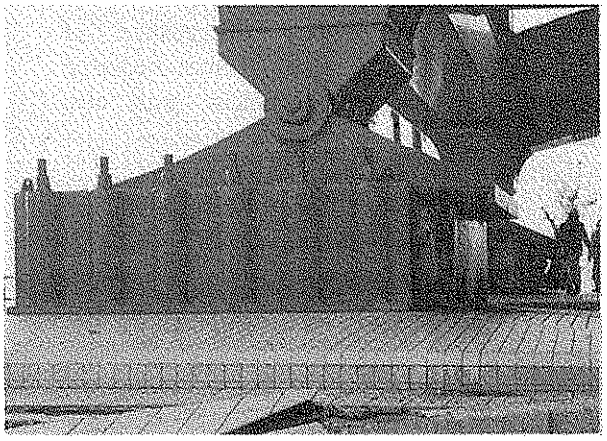

Photo 2 The damage at foundation P2

condition(Iai et al, 1992a). With the effective stress and strain vectors written by

$$\{\sigma'\}^T = \{\sigma'_x, \sigma'_y, \tau_{xy}\} \quad (1)$$

$$\{\varepsilon\}^T = \{\varepsilon_x, \varepsilon_y, \gamma_{xy}\} \quad (2)$$

the basic form of the constitutive relation is given by

$$\{d\sigma'\} = [D](\{d\varepsilon\} - \{d\varepsilon_p\}) \quad (3)$$

in which

$$[D] = K\{n^{(0)}\}\{n^{(0)}\}^T + \sum_{i=1}^{I} R^{(i)}_{L/U}\{n^{(i)}\}\{n^{(i)}\}^T \quad (4)$$

In this relation, the term $\{d\varepsilon_p\}$ in Eq.(3) represents the additional strain incremental vector to take the dilatancy into account and is given from the volumetric strain increment due to the dilatancy as

$$\{d\varepsilon_p\}^T = \{d\varepsilon_p/2, d\varepsilon_p/2, 0\} \quad (5)$$

The first term in Eq.(4) represents the volumetric mechanism with rebound modulus K and the direction vector is given by

$$\{n^{(0)}\}^T = \{1,1,0\} \quad (6)$$

The second term in Eq.(4) represents the multiple shear mechanism. Each mechanism i = 1,2,...,I represents a virtual simple shear mechanism, with each simple shear plane oriented at an angle $\theta_i/2 + \pi/4$ relative to the x axis. The tangential shear modulus $R^{(i)}_{L/U}$ represents the hyperbolic stress strain relationship with hysteresis characteristics. The direction vectors for the multiple shear mechanism in Eq.(4) are given by

$$\{n^{(i)}\}^T = \{\cos\theta_i, -\cos\theta_i, \sin\theta_i\}$$

(for i=1,2,...,I) (7)

in which

$$\theta_i = (i-1)\Delta\theta \quad \text{(for i=1,2,...,I)} \quad (8)$$

$$\Delta\theta = \pi/I \quad (9)$$

A schematic figure for the multiple simple shear mechanism is shown in Fig. 2. Pairs of circles indicate mobilized virtual shear strain in positive and negative modes of compression shear(solid lines with darker hatching) and simple shear(broken lines with lighter hatching).

The loading and unloading for shear mechanism are separately defined for each virtual simple shear mechanism by the sign of $\{n^{(i)}\}^T\{d\varepsilon\}$. The multiple shear mechanism takes into account the effect of rotation of principal stress axis directions, the effect of which is known to play an important role in the cyclic behavior of anisotropically consolidated sand(Iai et al 1992b). There are ten parameters in the present model, two of which characterize elastic properties of soil; another two specify plastic shear behavior, and the rest characterize dilatancy.

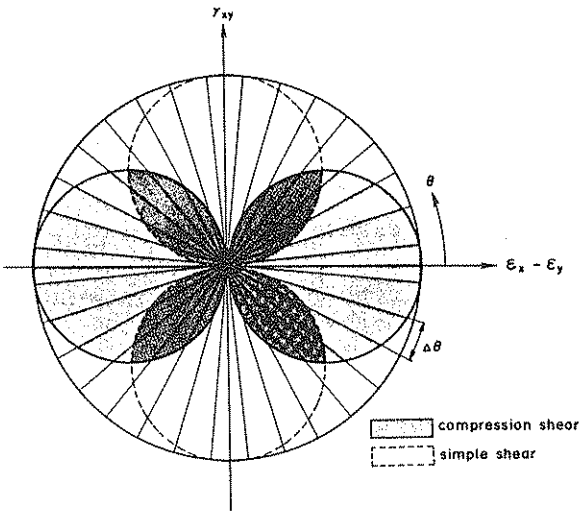

Fig. 2 Schematic figure for multiple simple shear mechanism

2.2 Finite Element Modeling

The finite element mesh shown in Fig.3 was used for the analysis of Kobe Ohashi Bridge under plane strain condition. Total of 2660 nodal points and 4654 elements were used. Five types of elements were used in the analysis, those were linear elements for caisson, nonlinear elements

for sand and clay; beam elements for the upper structure of bridge, liquid elements for water and joint elements for the boundaries between a soil and a structure. The sea water was modeled as incompressible fluid and was formulated as an added mass matrix based on the equilibrium and continuity of fluid at the solid-fluid interface (Zienkiewicz,1977).

2.3 Model Parameters

The model parameters were calibrated by referring to the in-situ velocity measurements and other relevant test results. Shown in Fig.4 were the results of the geotechnical investigations at the Fourth Pier and the Port Island in the vicinity of Kobe Ohashi Bridge.

The dilatancy parameters of fill soil and the sand replacing the original clay layer in Kobe Port were determined referring to Rokko Island data(Inagaki, et al.,1996). The dilatancy parameters for other soils were calibrated based on the SPT N-values and laboratory test results[Ministry of Transport, 1993]. The calibrated liquefaction resistance curves are shown in Fig.5. The computation parameters are shown in Table 1.

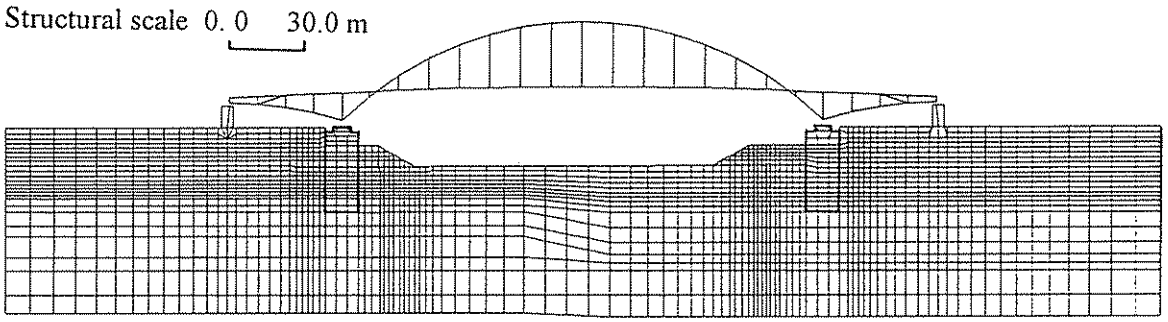

Fig.3 Finite element mesh for Kobe Ohashi Bridge

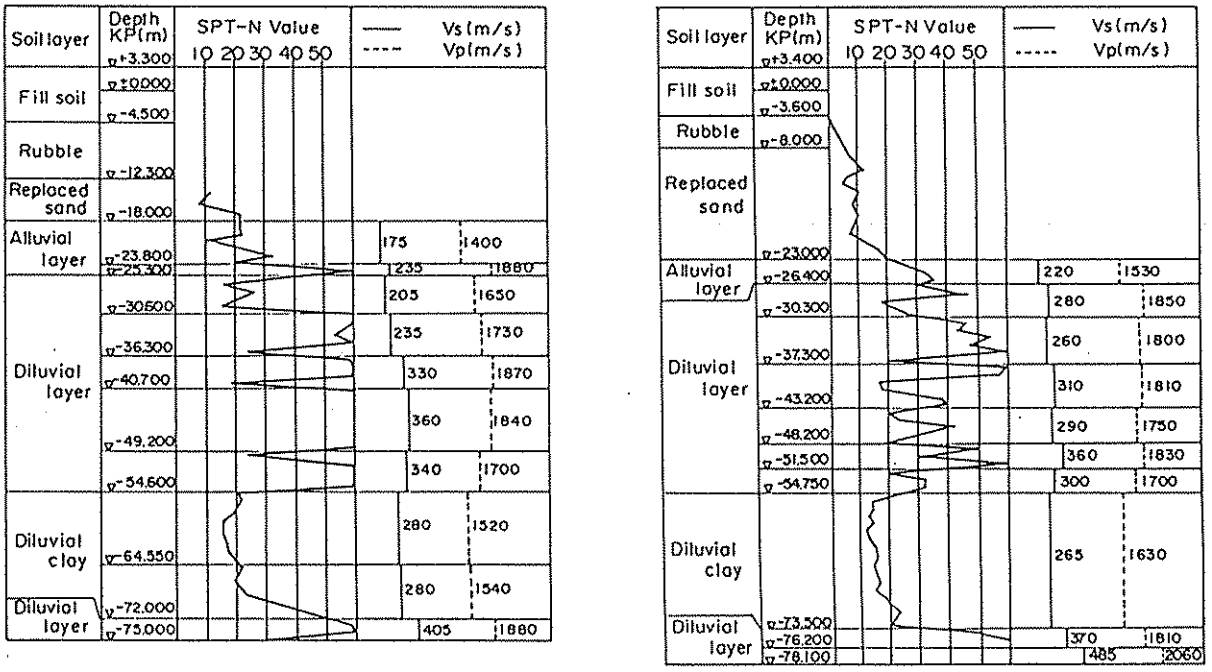

(a) The Fourth Pier (b) The Port Island

Fig.4 In-situ investigation results(After Okashita et al. 1996)

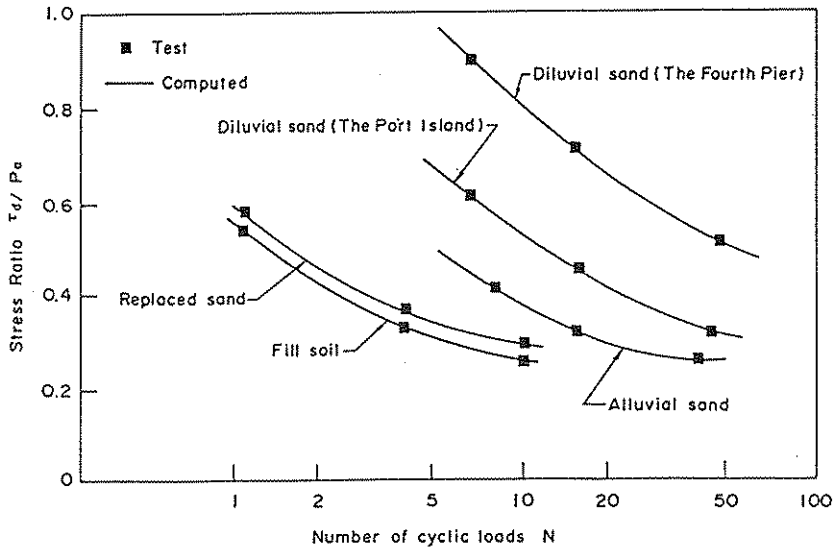

Fig.5 Computed liquefaction resistance curve

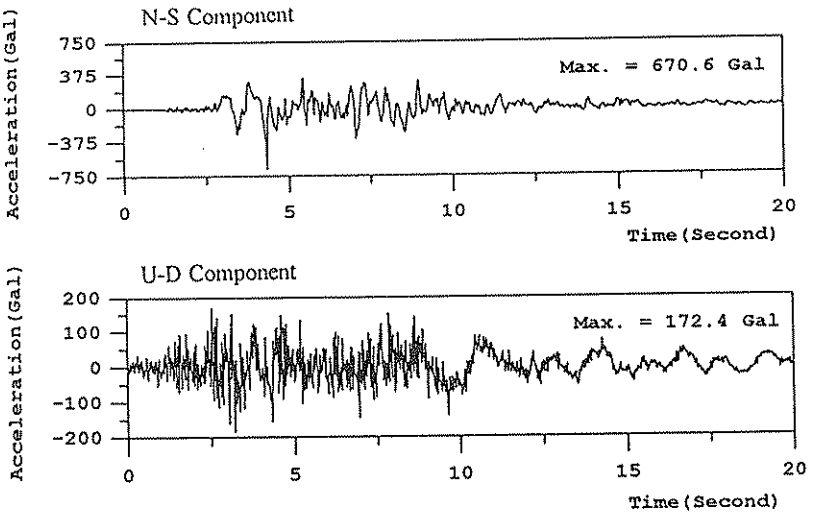

Fig.6 Earthquake motion at 1995 Great Hanshin earthquake recorded at 83 meters depth on Port Island

Table 1 Calculated parameters

Layer No.	γ (tf/m^3)	G_0 (tf/m^2)	K_0 (tf/m^2)	$-\sigma_m$ (tf/m^2)	ϕ'_f (deg.)	ϕ'_p (deg.)	Dilatancy parameters S_1 w_1 p_1 p_2 c_1
Fill soil	1.80	8000	20928	6.300	36	28	0.005 10.5 0.5 0.6 3.40
Replaced sand	1.80	7400	19358	10.60	36	28	0.005 5.50 0.6 0.8 2.30
Alluvial layer	1.96	6100	15958	14.67	36	28	0.005 16.0 0.5 0.8 2.50
Diluvial layer(1)*	1.89	17000	44472	25.00	40	28	0.005 145. 0.5 0.6 25.3
Diluvial layer(2)*	1.87	21000	54936	25.00	40	28	0.005 16.5 0.5 0.8 3.43
Replaced stone	1.92	18000	47088	22.27	40		
Clay layer	1.62	12000	31392	36.30	30		

* Diluvial sand layer(1) is in the Fourth Pier and Diluvial sand layer(2) is in the Port Island.

2.4 Input Accelerations

The earthquake motions were recorded with a vertical seismic array in the Port Island at the ground surface and at depths of 16 m, 32 m and 83m.during January 17,1995 Great Hanshin earthquake. The recording was successfully operated by the Development Bureau of Kobe City.

The site of vertical seismic array is very close to the Kobe Ohashi Bridge with only a distance about 150m. The records at the depth of 83 m shown in Fig. 6 was used as the bedrock motion in the effective stress analysis. The maximum horizontal acceleration in N-S direction is 670.6Gal, while the maximum vertical acceleration is 172.4Gal. It was noted in here that, though the orientation error of seismograph at the depth of 83m was existence(Sugito et al. 1996), the original data was used in this study.

Before the dynamic response analysis, a static analysis was performed to simulate the stress distributions to take the effect of gravity into account. The same constitutive model was used as in the earthquake response analysis but under drained condition. With these initial conditions and the parameters mentioned earlier, an earthquake response analysis was performed on the Kobe Ohashi Bridge. The analysis was conducted with the undrained conditions (Zienkiewicz et al. 1982) in order to simplify the analysis. The numerical time integration was made using of Wilson-θ method (θ=1.4) with the time interval of 0.01 seconds. Rayleigh damping (α=0 and β=0.005) was used to ensure the stability of numerical solution process.

3. RESULTS OF ANALYSIS

The results of the effective stress analysis of the Kobe Ohashi Bridge were shown in Figs. 7 and 10. Shown in Fig. 7 was the displacement and acceleration responses of Nodes 764 and 1658 at the top of caissons P2 and P3 indicated in Fig.8(a).

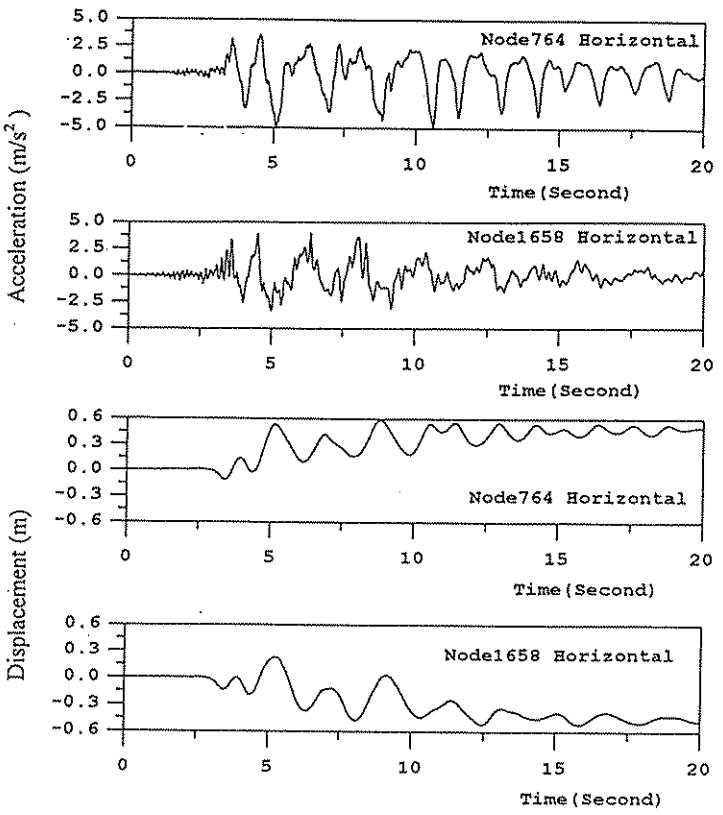

Fig. 7 Time history of deformation and acceleration

The displacements were gradually increased for about 15 seconds and then stayed closed to at the residual values. The shape and vectors of deformation at the end of the earthquake was shown in Fig.8(in figure, the deformation is scaled five as large for the plotting). It was seen that the deformation in the foundation was mainly around the caissons and both of two sides moved toward the sea. The predicted and measured results for the caissons are summerized in Table 2. The computed horizontal displacements were 0.46 m at P2 and 0.48 m at P3 while the settlement were 0.12 m and 0.11 m respectively, the total relative horizontal displacement was 0.94 m. The order of computed deformation was consistent well with the measured after earthquake.

To evaluate the degree of liquefaction of the foundation, the excess pore water pressure ratio specified in terms of $(1-\sigma'_m/\sigma'_{m0})$ was computed, where σ'_m, σ'_{m0} were the current and initial mean effective stresses. The time histories of pore water pressure ratios of elements 384, 1819 in the fill soil and elements 710, 1463 in the replaced sand indicated in Fig.10 were shown in Fig. 9. The pore water pressure were gradually increased to the ratio of 0.85 for about seven seconds and then remained at the high values until the end of earthquake. The residual displacements in Fig.7 were increased with the developement of excess pore water pressure. Distribution of the computed excess pore water pressure ratio contour at the end of the earthquake is shown in Fig. 10. It appeared that liquefaction occurred in the fill soil and replaced sand, these high excess pore water pressures may have affected the performance of the pneumatic caissons for the Kobe Ohashi Bridge.

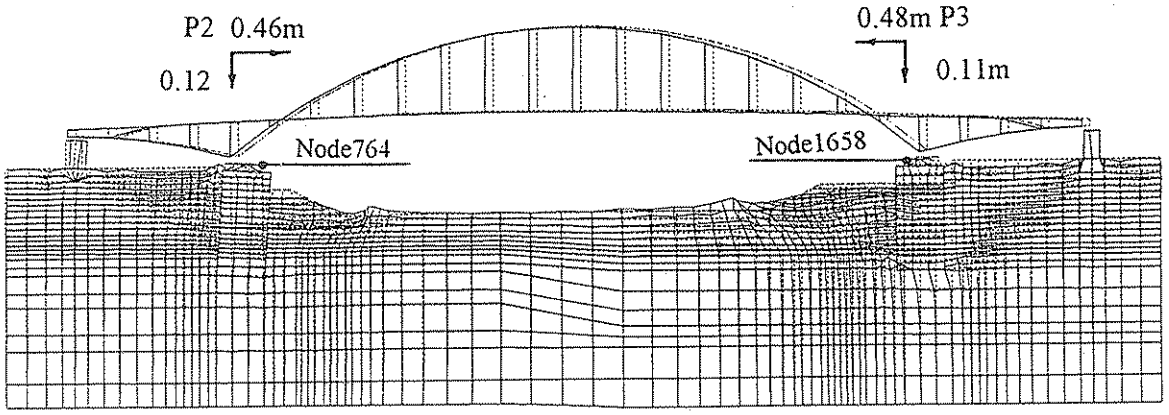

(a) The shape

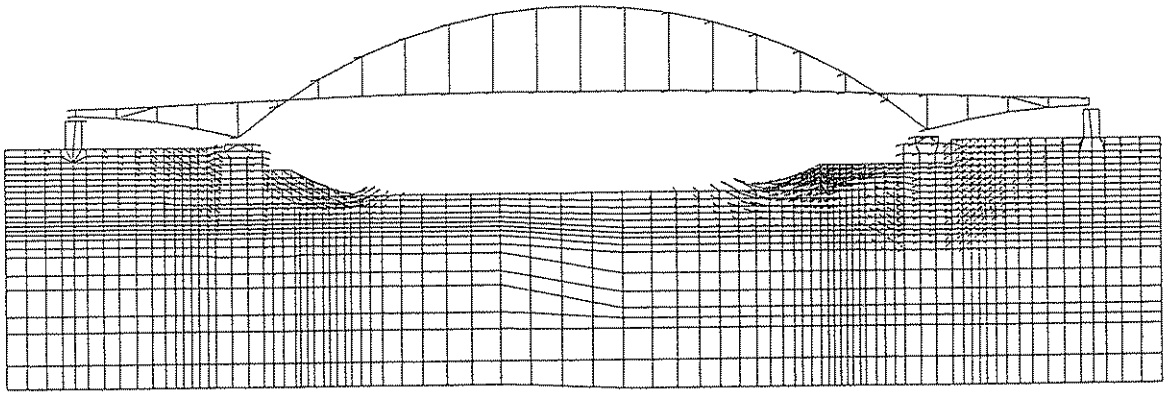

(b) The vectors

Fig. 8 The shape and vectors of computed deformation(main part)

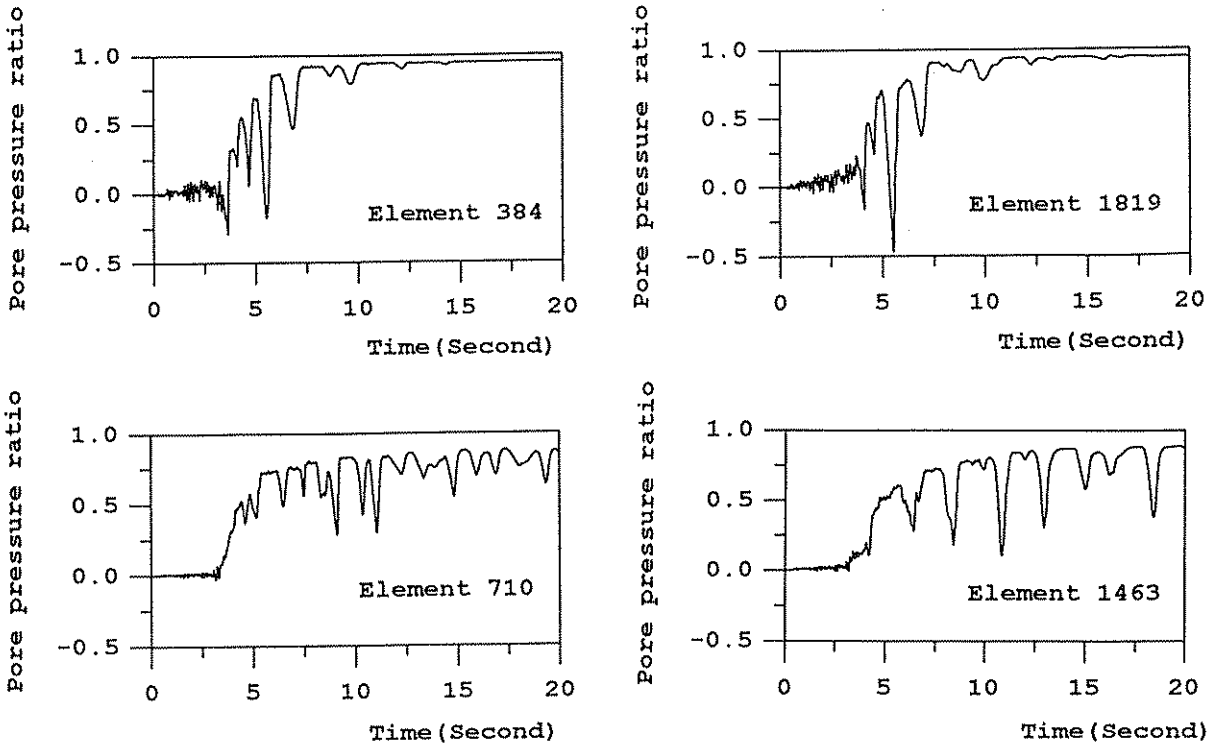

Fig. 9. Time history of excess pore water pressure ratio

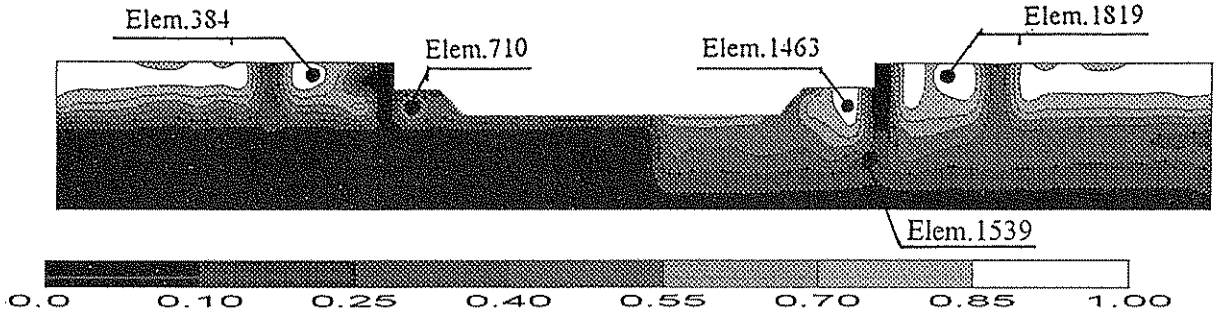

Fig. 10. The computed excess pore water pressure ratio

Table 2 The results for caissons

Items	Caisson	P2	P3
Horiz. disp (m)	Compu.	0.46	0.48
	Measu.	Total:	0.60 - 0.80
Incl. angle (deg.)	Compu.	0.68	0.07
	Measur.	0.36 - 0.73	0.78 - 0.93

4. MECHANISM OF DEFORMATION

In order to look into the mechanism of deformation of pneumatic caisson foundations, the stress and strain of soils in the upper fill soil and in the diluvial layer of Port Island indicated by element 384 and 1539 in Fig.10 were plotted in Fig.11. In the fill soil, the effective stress path rapidly decreased and closed to the original as shown at the bottom in Fig.11(a). In accordance with this, the axial strain difference was gradually induced as shown in the upper row of the same figure and the magnitude of the shear strain γ_{xy} in the upper fill was relatively small.

It can also be seen from Fig.11(b) that, in the diluvial layer of Port Island, the effective stress path gradually approached the failure line with fluctuation around the initial deviatoric stress. Even the effective mean stress was once decreased 35 percent, the final value, however, is 220KPa. In accordance with this, the axial strain difference was gradully induced as shown in the middle row of the same figure. The shear strain γ_{xy} was also gradually induced but with a relatively small value. As a result, the deformation of pneumatic caisson foundation was likely to be induced due to the existence initial stress and its release in accordance with overall softening of saturated soil with the mechanism of cyclic mobility.

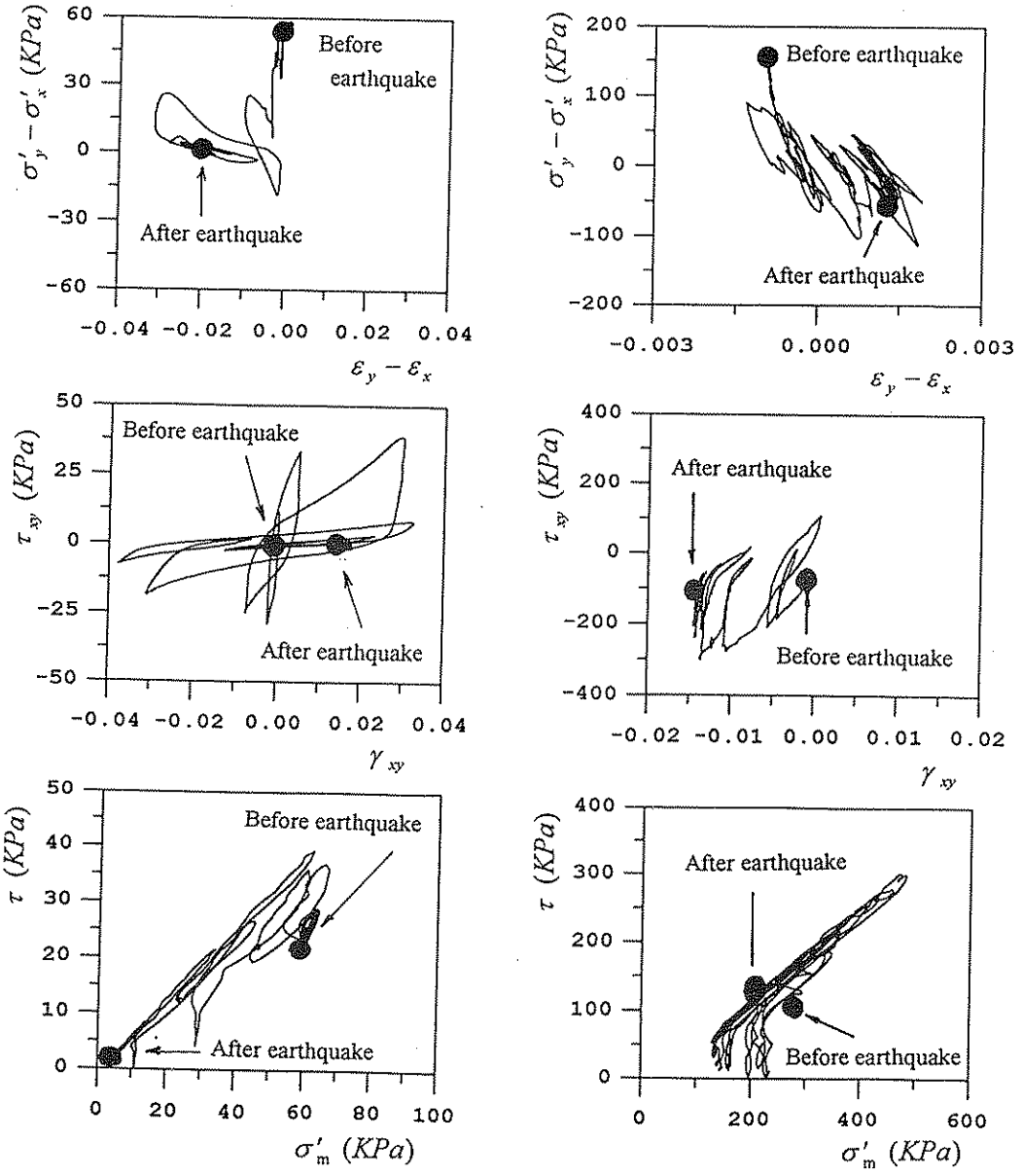

(a) In fill soil (b) In diluvial layer of Port Island

Fig.11 Predicted stress strain relation and stress path

5. INFLUENCE OF EXCESS PORE WATER PRESSURE

In order to evaluate the effect of the excess pore water pressure increase in the foundation, the following three cases of analyses were performed by introducing an artificial soil model, to be called non-liquefiable soil model which has the same properties as those used in the aforementioned analysis but completely lacks the characteristics of dilatancy. The case which dealt with the actual bridge foundation during the earthquake shown in the previous is designated as Case-1. Case-2 is to idealize both the upper fill and the diluvial layer were the non-liquefiable soils. Case-3 is to idealize only upper fill was non-liquefiable, and Cases-4 is to idealize only diluvial layer was non-liquefiable.

In order to quantify the individual effect of excess pore water pressure increase in the upper fill and diluvial layer, the principal results of the deformation were summarized in Table 3 including those of Case-1. The excess pore water pressure distribution for case-2 to 4 were shown in Fig.12. The results of Case-2 shown that the seaward displacement was 0.31m at the top of a caisson while 0.17m at the top of the other caisson, and resulting in a total of only 0.48m induced purely due to the inertia force of the earthquake. Therefore, it was revealed that the excess pore water pressure increasing in the foundation was to increase the displacement about 2 times as those induced purely by the inretia force due to the earthquake. When there is no effect of excess pore water pressure increase in the foundation, deformation becomes quite localized around the caisson foundation in case-2. The result of Case-3 shown that the excess pore water pressure increase in the upper fill and replaced sand will increase the deformation of caisson about 1.5 times of those induced in Case-2. It is speculated that the soil improvement in the upper soil can restrain the displacement of caisson foundation. The excess pore water pressure increase in the diluvial layers under the caisson P3 as shown in Case-4 was to increase the displacement about 20 percent of those induced in Case-1. It was also noted from Fig.9(a) that the shear deformation under caisson foundation P3 was far larger than that under caisson foundation P2, so the reason was speculated due to the high excess pore water pressure occured in the diluvial layer.

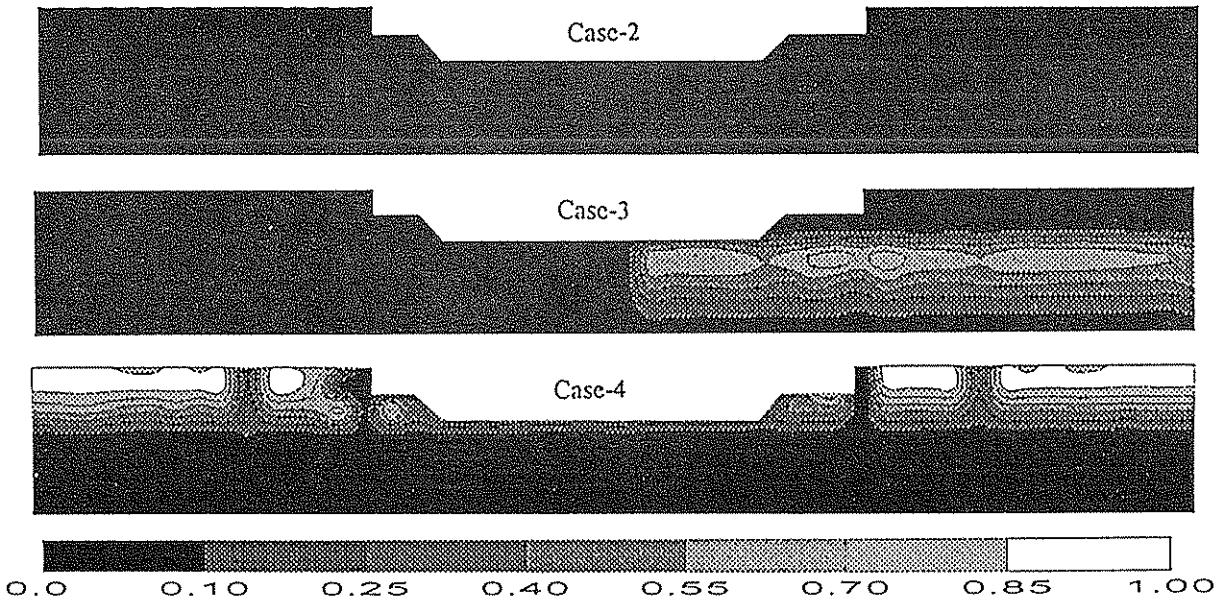

Fig.12 Computed excess pore water pressure for Case-2 to 4

Table 3 Computed residual displacement

Case	P2(m)	P3(m)	Total(m)
Case-1	0.46	0.48	0.94
Case-2	0.31	0.17	0.48
Case-3	0.28	0.34	0.62
Case-4	0.46	0.16	0.62

6. SOIL IMPROVEMENT ANALYSIS

For the safety operation of bridge, the soil improvement was taken around the caisson by the Kobe city after earthquake. The High Pressure Jet Grouting scheme and Gravel Pile scheme were used to improve the strength and liquefaction resistance of soil. The areas of improvement were shown in Fig.13(Okashita et al. 1996).

In order to evaluate the effectiveness, the analysis for the improved foundation was conducted in here. The same cross section as shown in Fig.1 but partly material parameters changed and the same input motions indicated in Fig. 7 were used for the post improvement analysis. The parameters for improved area was shown in Table 4. Fig.14 was the computed residual displacement. The computed horizontal residual displacement were 0.19m on the top of caisson in the Fourth Pier and 0.39m in the Port Island, respectively resulting in a total of 0.58m total deformation which reduced about 38 percent with the un-improvement case. The settlements at both of two sides reduced to 0.04 m. The comparison of results was shown in Table 5. Fig.15 was the distribution of excess pore water pressure ratio.

Comparing to Fig.10, the excess pore water pressure around the caissons was restrained, and the range of liquefaction was reduced obviously, so the soil improvement after earthquake was effective and reasonable.

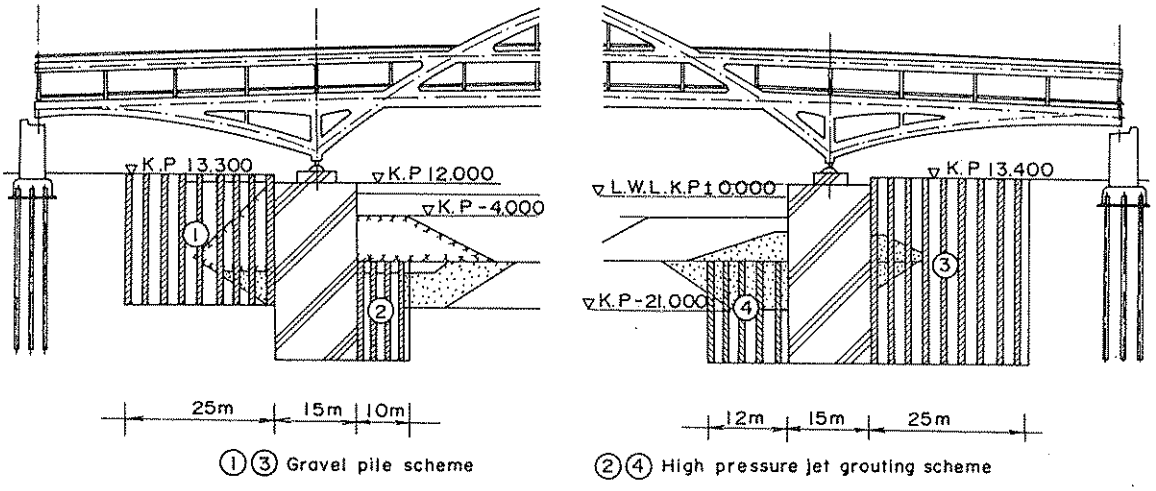

(a) In the Fourth Pier side

(b) In the Port Island side

Fig.13 Soil improvement area

Table 4 Parameters for improved areas

Soil No.	γ (tf/m^3)	G_0 (tf/m^2)	K_0 (tf/m^2)	$-\sigma_m$ (tf/m^2)	ϕ'_f (deg.)
①	1.80	8800	23020	6.430	40
②	1.80	10600	27730	14.67	40
③	1.80	8800	23020	6.430	40
④	1.80	10600	27730	14.67	40

Table 5 The computed displacement for improvement

	Improvement	P2	P3
Horiz. disp. (m)	Before	0.46	0.48
	After	0.19	0.39
Vertical disp. (m)	Before	0.12	0.11
	After	0.04	0.04
Prone angle (deg.)	Before	0.68	0.07
	After	0.28	0.07

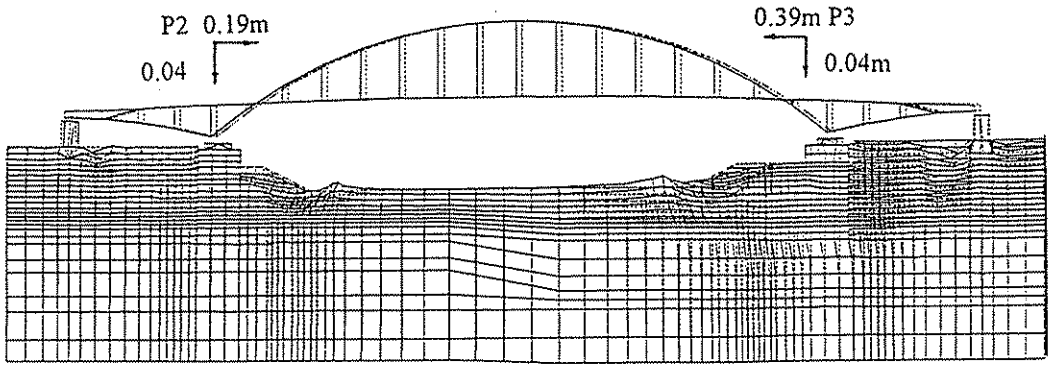

Fig.14 Computed residual deformation after improvement

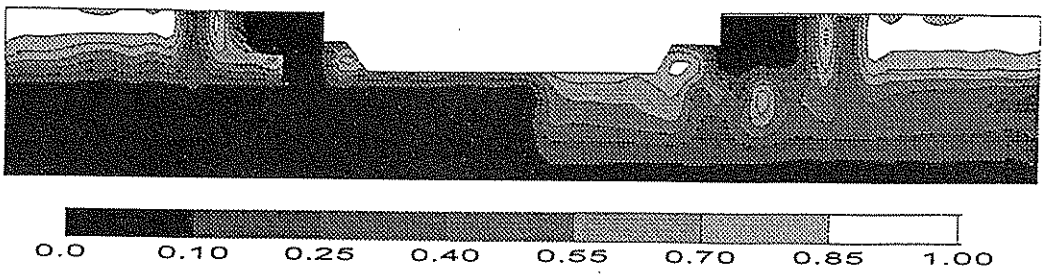

Fig.15 Computed excess pore water pressures after improvement

7. CONCLUSIONS

The effective stress analysis was performed for the Kobe Ohashi bridge during the 1995 great Hanshin earthquake, and led to the following conclusions.

The computed horizontal displacements were 0.46 m on a caisson in the Fourth Pier and 0.48 m on another caisson in the Port Island, the total seaward displacement was 0.94 m. The settlements were 0.12m and 0.11m at P2 and P3 respectively. The order of computed displacement was in good agreement with the measured after earthquake.

Under the earthquake excitation, the pore water pressure increased in the foundation and may have affected the performance of the pneumatic caisson. The excess pore water pressure increasing in the fill soil increased the deformation of pneumatic caissons about two times as large as that purely caused by the seismic inertia force. It was also found that the excess pore water pressure increasing in the diluvial sand layer of Port Island result bigger

shear deformation at the bottom of caisson. The deformation of pneumatic caisson foundation was likely to be induced due to the existence of release in accordance with overall softening of saturated soil with the mechanism of cyclic mobility.

After ground improvement, the computed horizontal residual displacement were 0.19m on the top of caisson in the Fourth Pier and 0.39m in the Port Island, respectively, the total of seaward displacement was 0.58m which was reduced by 38 percent, the excess pore water pressure increasing around the caisson is constrained, so the effect of ground improvement was confirmed.

Based on the above analysis, it was also concluded that, the present model used in the paper has the potential ability to simulate the characteristics of deformations of pneumatic type foundation under strong earthquake motion.

ACKNOWLEDGMENT

The authors gratefully acknowledge the Kobe City for kindly permitting the use of data relevant to the Kobe Bridge. The supports of the STA Fellowship of Japan is also acknowledged.

REFERENCES

1) Editorial Committee for the Report on the Hanshin-Awaji Earthquake Disater, 1996, Damage to Civil Engineering Structures, Bridge Structures. 283-286(in Japanese)
2) Iai, S., Matsunaga, Y and Kameoka, T 1992a, Strain space plasticity model for cyclic mobility, Soils and Foundations, Vol.32, No.2, pp.1-15
3) Iai, S., Matsunaga, Y and Kameoka, T 1992b, Analysis of cyclic behavior of anisotropically consolidated sand, Soils and Foundations, Vol.32, No.2, pp.16-20
4) Inagaki, H., Iai, S., Sugano, T., Yamazaki, H., and Inatomi, T. 1996, Perfor-mance of caisson type quey walls at Kobe port, Soils and Foundations, Special Issue. pp.119-136
5) Inatomi, T., Zen, K., Toyama, S., etc., 1997, Damage to port-related facilities by 1995 Hyogoken-nanbu earthquake, *Technical Note of the Port and Harbour Research Institute*, Ministry of Transport, Japan, 857
6) Japan Architecture Association, 1988, Handbook of Structural design of architecture foundation, pp.163-169
7) Ministry of Transport ed. 1993, Handbook for Liquefaction remediation of reclaimed land, pp.243-245(in Japanese)
8) Okashita, K., Okutani S., Ojima S., and Fujita, C., Numerical study on seismic damage of caisson foundations due to ground liquefaction and examination of countermeasures. Proc. of Civil Engineer Society of Japan on Great Hanshin-Awaji Earthquake, Tokyo, pp.611-618(in Japanese)
9) Sugito, M., Sekiguchi, K., Yashima, A. , Oka, F., Taguchi.Y and Kato, Y. 1996, Correction of orientation error of borehole strong motion array records obtained during the South Hyogo Earthquake of Jan.17, 1995, *Journal of Structural Mechanics and Earthquake Engineering*, JSCE, 12(3 and 4), pp.51-63
10) Yoshimi, Y. 1991, Liquefaction on Sand Foundation, Gihoudo Press, 2nd edition, pp.86(In Japanese)
11) Zienkiewicz, O.C. 1977, The Finite Element Method, 3rd edition, McGraw-Hill Book Co.
12) Zienkiewicz, O.C. and Bettess, P. 1982, Soils and other saturated media under transient, dynamic load conditions, Soil Mechanics-Transient and Cyclic Loads, Pande & Zienkiewicz eds., John Wiley and Sons, pp.1-16